J. Fluid Mech. (1983), *vol.* 127, *pp.* 453–472
Printed in Great Britain

Shear stresses developed during rapid shear of concentrated suspensions of large spherical particles between concentric cylinders

By STUART B. SAVAGE AND SHAWN McKEOWN
Department of Civil Engineering and Applied Mechanics, McGill University, Montreal, Canada

(Received 25 June 1980 and in revised form 9 September 1982)

Experiments were performed on concentrated suspensions of large (0·97–1·78 mm mean diameters) neutrally buoyant spherical particles sheared in a concentric-cylinder Couette-flow apparatus in which the inner cylinder rotated while the outer one was fixed. The variations of shear stress with apparent shear rate, concentration, particle diameter and wall roughness were studied, and the results are compared with related experiments of Bagnold. Generally the shear stresses measured in the present experiments were larger than those of Bagnold. The difference can be attributed to differences in the experimental arrangements; Bagnold's flexible-walled inner cylinder was fixed while the outer cylinder rotated. A strong effect of wall roughness was observed. The higher stresses generated with rough walls imply that particle 'slip' may have occurred in the smooth wall tests. The larger stresses might also be due to an increase in strength of the interparticle collisions caused by the roughness. No dependence of stress upon particle diameter d was observed for concentrations of about 0·3, but a strong dependence ($> d^2$) was found at the highest concentrations with the rough walls.

1. Introduction

The rheology of concentrated suspensions of large solid particles in liquids at high shear rates is of interest in connection with a broad range of flows; for example, the hydraulic transport in pipelines of particulate solid materials such as coal, mineral concentrate and animal feeds, bedload sediment transport in streams, sediment gravity flow in the deep ocean, debris flows and flows in fluidized beds.

One of the earliest and most extensive experiments dealing with such flows was performed by Bagnold (1954). This work was motivated by an interest in the mechanics of phenomena such as sediment transport occurring at river beds. By using a flexible rubber inner cylinder wall in his co-axial rotating-cylinder Couette-flow apparatus Bagnold could measure both the torque and the normal stress in the radial direction when various concentrations of neutrally buoyant spherical particles were sheared by rotating the rigid outer cylinder. Bagnold defined three flow regimes depending upon the value of a dimensionless shear rate group which was analogous to a conventional Reynolds number. In his *macro-viscous* regime, corresponding to low shear rates where fluid viscosity is important, the stresses are linearly proportional to the shear rate. In the high-shear-rate *grain-inertia* regime, he proposed that the interstitial fluid plays a minor role and that the main contributions to the stresses could be attributed to interparticle friction and collisions. In this region both the normal stresses and the shear stresses depend upon the square of the shear rate. Joining these two limiting regions is a *transitional* region where the effects of both

fluid viscosity and grain inertia are important. Bagnold also provided simple theoretical arguments to explain the rheological behaviour in the various flow regimes.

More recent literature dealing with concentrated suspensions has been reviewed by Jeffrey & Acrivos (1976) and Gadala-Maria (1979). Most of the papers they discussed pertain to small particles at low Reynolds numbers and few of them dealt with dense suspensions of large particles at high shear rates. As Bagnold discussed, these latter flows behave very differently from dilute suspensions at low Reynolds numbers; their rheological behaviour is more akin to that familiar in soil or powder mechanics when a bulk made up of dry granular material is deformed. For this reason Cheng & Richmond (1978) have termed the rheological behaviour of these dense suspensions as 'granulo-viscous'. In viscometric experiments typically one may observe (Cheng & Richmond 1978):

(*a*) the development of normal stresses proportional to the shear stress;

(*b*) dilation and compaction of the particles depending upon the normal stresses and shear rates;

(*c*) formation of rigid no-flow zones and shear bands;

(*d*) fluctuations in the measured stresses associated with the jamming, locking and release of particles;

(*e*) step-like changes in flow stresses, most likely arising from sudden changes in the arrangement of particle arrays;

(*f*) different stress *vs.* strain-rate curves depending upon whether the stress measurements correspond to a loading or an unloading sequence; and

(*g*) significant wall effects when the ratio of particle diameter to viscometer wall separation is not small.

While these phenomena have been identified, the mechanics governing them are poorly understood. Many arise because of the finite size of the particles and the shear gap of the viscometer. These finite-size effects can be frustrating to the experimentalist, as they cause 'scatter' in the experimental data and make the results difficult to interpret. It is not always clear whether the measurements reflect the properties of the 'granular fluid' or those associated with the test apparatus. There is a strong need for further experimental data to stimulate and guide the theoretical treatment of rapidly sheared dense suspensions.

The object of the present experimental study was to extend Bagnold's (1954) tests by investigating the effects of varying the particle size and the shear cell wall roughness and rigidity (Bagnold tested only one particle diameter in a shearing apparatus that had smooth walls, one of them flexible), and to determine the results of rotating the inner cylinder rather than the outer one. Measurements of shear stress versus shear rate for various concentrations of neutrally buoyant spherical particles are presented. At the outset of this investigation it was our aim to determine distinct 'viscosity coefficients' as one might do for a laminar non-Newtonian fluid. As a result of the present and other studies, we now regard this aim to some extent as naive, in the same sense that the idea of a definitive value for the eddy viscosity for a turbulent Newtonian fluid is naive. The results of the present experiments are compared with Bagnold's (1954) data and possible reasons for the differences are discussed with the recognition that things are rather more complicated than suggested in Bagnold's pioneering work.

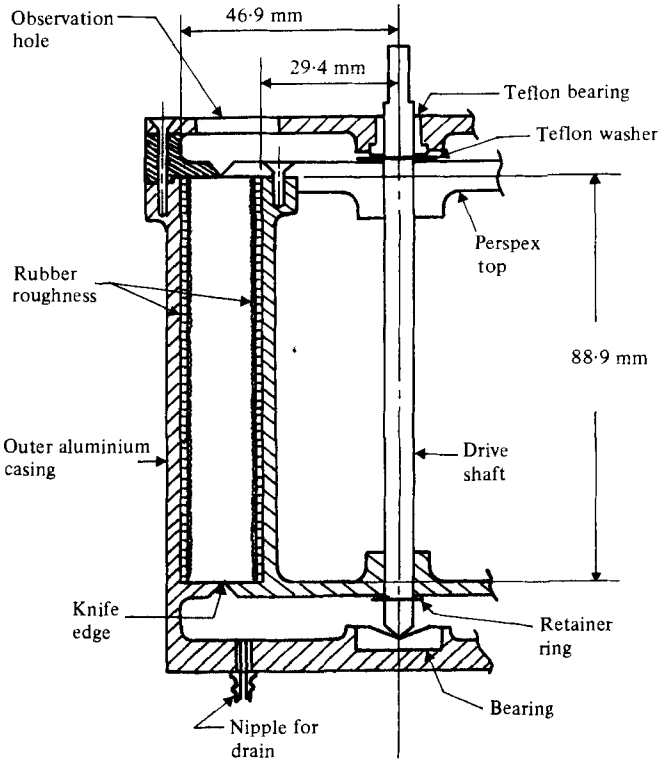

FIGURE 1. Coaxial rotating-cylinder Couette-flow device.

2. Apparatus and experimental procedures

2.1. *Couette-flow device*

A concentric-cylinder Couette-flow shear cell (figure 1) was designed so that it could be used in conjunction with the torque-loading mechanism of a commercially available Stormer viscometer (Thomas Viscometer no. 15-348, available from Fisher Scientific Co. Ltd, Montreal). A photograph of the test set-up is shown in figure 2. The suspensions were sheared in the annular space between the two concentric cylinders, the outer one being fixed and the inner one rotating and driven by a falling weight. The driving mechanism consists of a weight Mg, which turns a pulley of radius $R = 14{\cdot}3$ mm causing an input torque to the system of MgR. Between this pulley and the drive shaft of the inner cylinder there is a gearbox which increases the rotation rate of the inner cylinder by a factor of 11 and reduces the torque by $\frac{1}{11}$. Thus the driving torque on the inner cylinder $T_d = \frac{1}{11}MgR$. In the steady state, the driving torque T_d equals the resisting torque T_r developed by the sheared suspension. The resisting torque may be expressed as $T_r = 2\pi r^2 L\tau$, where L is the length of the annular shear region and τ is the shear stress developed at radius r by the suspension. By equating the driving and resisting torques the shear stress can be related to the driving weight as follows:

$$\tau = \frac{MgR}{22\pi r^2 L}. \tag{1}$$

The drive system has a counter that registers the number of revolutions which the inner cylinder makes. The angular velocity of the inner cylinder was determined by measuring the time increment taken for a given number of revolutions. The beginning

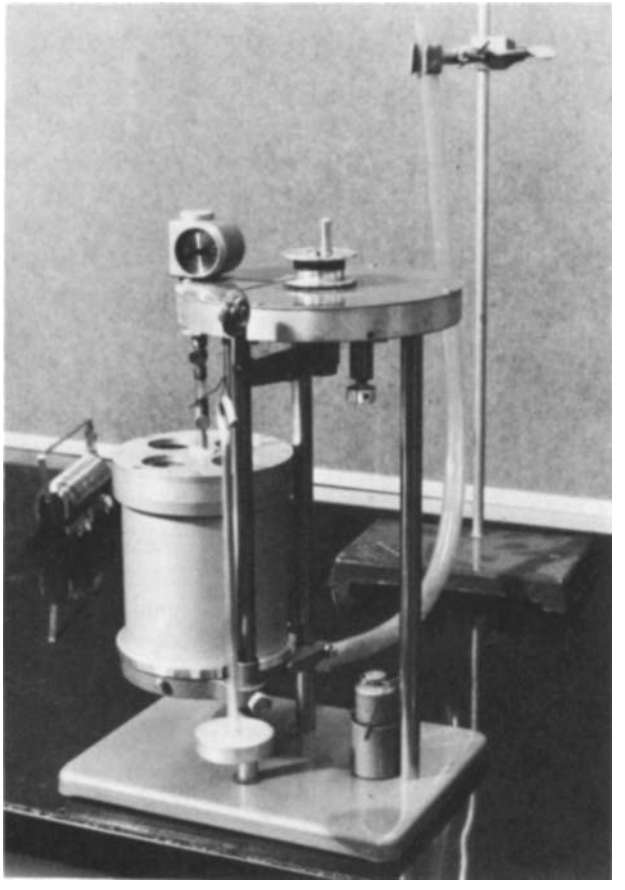

FIGURE 2. Photograph of experimental apparatus.

in real time of each time increment was entered into the McGill 'Datac' Computer through a remote terminal. This gave a running check on whether steady-state conditions in the viscometer were reached. In general, the steady-state velocity (which corresponds to successive time increments being equal) was reached very quickly.

Tests were performed with the vertical cylindrical walls of the annular shear region in both a smooth and a roughened state. For the smooth-wall tests the inner and outer aluminium cylinders were polished and anodized to give hard and smooth surfaces. In this case the inner and outer cylinder had outer and inner diameters of 58·8 and 93·8 mm respectively, giving an annular shear space 17·5 mm wide and 88·9 mm high.

To investigate the effects of wall roughness, rough rubber sheet (figure 3) was glued directly to the existing outer and inner cylinder walls. Rubber roughness was chosen so that no damage would occur to either the particles or the shear cell if particle locking or jamming occurred during a test. The spacing and size of the short cylindrical protuberances that covered one side of the rubber sheet were of the same order as the diameters of the particles in the suspensions. With the rubber sheets attached, the diameters of the inner and outer cylinders corresponding to the tops of the roughness elements were 63·8 and 88·8 mm respectively, giving an annular gap between the tops of the roughness elements of 12·5 mm. The total volume of the annular shear cavity with the roughness attached was measured to be 0·293 litres.

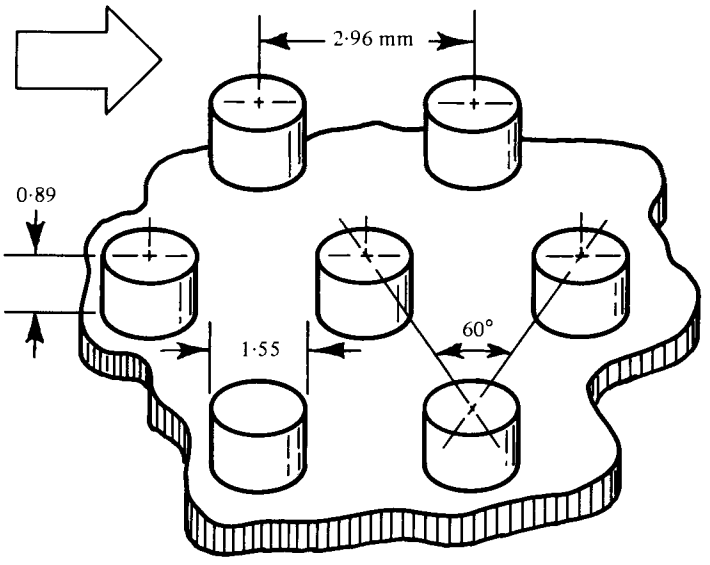

FIGURE 3. Geometry and dimensions of wall-roughness elements.

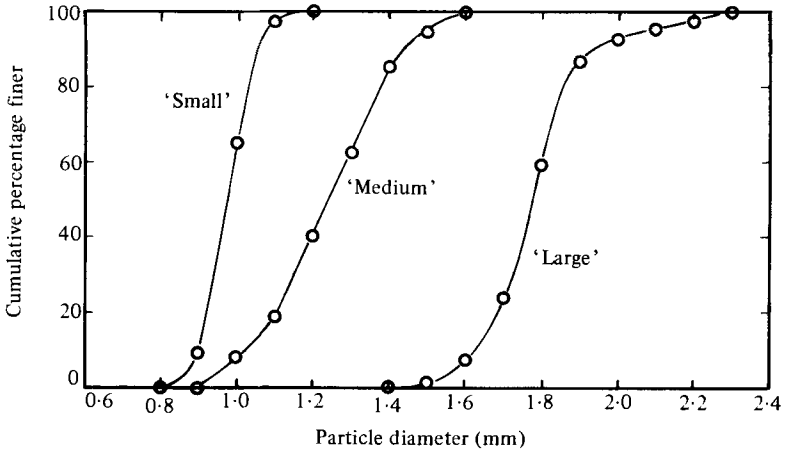

FIGURE 4. Particle-size distribution for 'small', 'medium' and 'large' diameter spherical polystyrene beads having mean diameters of 0·97, 1·24 and 1·78 mm respectively.

2.2. *Suspensions*

2.2.1. *Physical characteristics.* The solid particles used to form the suspensions were spherical polystyrene beads having a density ρ_s of 1·029 g/cm^3. For low stress levels encountered in the tests the spheres may be regarded as rigid. Three groups of beads were segregated from a broad-ranged raw sample by sieving. The mean diameters d of the three smaller samples were 0·97, 1·24 and 1·78 mm. The size distributions (figure 4) for each of these samples were obtained by measuring the diameters of 75 spheres from each sample with a micrometer. The 'medium' (1·24 mm mean diameter) spheres had a broader size distribution than the 'small' (0·97 mm) or 'large' (1·78 mm) spheres. The quasi-static angle of friction between dry polystyrene beads and an aluminium surface similar to the *smooth* cylindrical walls was determined to be 14°. The internal angle of friction for the beads themselves was 24°.

The polystyrene beads were suspended in salt water having a specific gravity of 1·029, equal to that of the beads. The suspensions were loaded into the Couette device by filling the shear cell with salt water up to the level of the bottom of the shear space, preparing an amount of the desired concentration equal to the volume of the annular shear space, carefully pouring this mixture into the annular shear space and replacing the top assembly of the Couette device.

2.2.2. *Packing characteristics.* At high concentrations the shear stresses measured in the present experiments (which are discussed in §3) were higher than those measured by Bagnold (1954) in a somewhat similar apparatus. Also, in the present experiments, the beads locked together and could not be sheared at concentrations lower than those for which Bagnold was able to maintain continued shear. Bagnold's particles were 'uniform' wax beads of 1·32 mm diameter, whereas the beads used in the present experiments had the size distributions as shown in figure 4. The question arises as to whether these differences in experimental results are more likely due to differences in the particles (uniform diameter versus a distribution of particle sizes) or differences in the shear cells. We supposed that some idea of the significance of the particle size distributions might be obtained by comparing (i) the values of the concentration for a random dense packing with data for uniform-diameter spheres and (ii) the solids concentrations at 'fluidity' with Bagnold's (1954) value for uniform spheres.

The maximum solids fraction ν for random packing of each of the three sphere size ranges was determined by the methods proposed by Scott (1960). To eliminate container-wall boundary effects, measurements were made in a number of cylinders of different height and diameter, and the resulting values of ν were extrapolated to correspond to a container of infinite size. The values of ν thus obtained for dense random packing were 0·642, 0·644 and 0·641 for the 'small', 'medium' and 'large' spheres. Scott (1960) measured values of ν between 0·634 and 0·637. Using computer models, Finney (1970) has refined the maximum concentration for uniform spheres to 0·6366. Because of the size gradation manifest in the present polystyrene beads, the maximum solids concentration is slightly larger than the uniform sphere value (Brown & Richards 1970; Dexter & Tanner 1971). The 'medium'-sized spheres, being less uniform in diameter (figure 4), have a slightly higher maximum concentration than the 'small' and 'large' spheres.

A highly concentrated suspension of particles can lock together and behave as a solid mass, supporting a shear stress at zero shear rate. There is a value of the concentration corresponding to what Bagnold (1966) termed 'fluidity' where the residual shear resistance at zero shear rate disappears. Bagnold (1966) measured the solids fraction at 'fluidity' to be 0·60 for a suspension of wax spheres having very nearly uniform 1·32 mm diameters. The 'fluidity' concentrations for the present beads were determined by placing a beaker of dry beads on an essentially friction-free surface and adding salt water until no motion of the beaker could be observed when a vertical 6 mm diameter cylindrical rod was moved horizontally very slowly through the mixture. Solids concentrations at fluidity of between 0·605 and 0·61 were measured for the three (small, medium and large) bead sizes; these were close to Bagnold's value of 0·60 for uniform spheres. It should be noted that, in some shear-cell tests to be described later, it was found impossible to shear the suspension at a concentration of 0·602. Thus, although the mean concentration for fluidity is around 0·60, it is likely that the local concentration in the region of the stirring rod where shear occurs is rather lower than 0·60.

In conclusion, the similarities in the present values of ν for random dence packings and ν for fluidity with those values for uniform spheres suggest that the beads used

in the present experiments behaved much as if they were uniform in diameter. The spread in diameter for a given group of beads was too small to have much effect.

2.3. *Calibration*

When the inner cylinder of the Couette device is driven at a constant rotation rate, the resisting torque is made up of three contributions: (*a*) bearing friction and other components of mechanical machine drag; (*b*) fluid resistance due to the shearing of the salt water contained in the bottom cavity underneath the inner cylinder; and (*c*) resistance due to the suspension contained in the annular shear space. In his experiments, Bagnold (1954) separated the torque required to *shear the suspension* into two parts, one which he attributed to the grains alone, and the other due to the interstitial fluid. He determined the shear stress τ_f of the plain fluid ($\nu = 0$) in the shear space as a function of shear rate. The Reynolds numbers were such that the flow was always turbulent. He argued that increasing the grain concentration decreased the amount of interstitial fluid and also suppressed the turbulence in what was left. To obtain a rough approximation for the shear stress due to the grains alone, he subtracted from the total shear stress required to shear the suspension an amount $\tau_f/(1+\lambda)$, where λ is a 'linear concentration' equal to the ratio of the particle diameter to the mean free distance between particles. The solids fraction ν may be expressed in terms of λ as

$$\nu = \frac{\nu_\infty}{(1+1/\lambda)^3}, \tag{2}$$

where ν_∞ is the maximum possible concentration when $\lambda \to \infty$ (for spheres $\nu_\infty = \pi/3\sqrt{2} = 0{\cdot}7405$).

With the present shear cell, measurements of applied torque versus rotation rate were made with and without salt water in the apparatus. Figure 5 shows typical results for smooth walls reduced to the form of *equivalent* shear stress at the mid-radius of the annular shear space ($r_m = 38{\cdot}15$ mm) versus the apparent shear rate $\omega r_i/(r_o - r_i)$, where ω is the angular velocity of the inner cylinder and r_i and r_o are the inner and outer radii of the annular shear space. (The torques, *which may include machine friction*, may be expressed in terms of an effective or *equivalent* shear stress acting at the mid-gap radii.) Assuming that the bearing and machine friction remain unchanged between tests with and without salt water, the difference between the two tests (see curves 1, 2 and 3 of figure 5) should correspond to the torque required to shear the fluid.

Bilgen & Boulos (1973) have performed experiments in which fluid was sheared in a concentric-cylinder Couette device by rotating the inner cylinder. They compared their results with those of several other investigators and presented correlations of moment coefficient C_m as functions of a Couette Reynolds number Re and ratio $(r_o - r_i)/r_i$ of gap to inner radius, where

$$C_m = \frac{T_d}{\frac{1}{2}\pi\rho\omega^2 r_i^4 L}, \quad Re = \frac{\rho\omega r_i(r_o - r_i)}{\mu}, \tag{3}$$

and ρ and μ are the fluid density and viscosity. By making use of these correlations for the ratio of annular-gap thickness to inner-cylinder radius appropriate for the present smooth-wall apparatus, we have calculated the shear stress (at mid-gap) as a function of apparent shear rate and shown it as curve 4 in figure 5. It may be seen that the stresses given by curve 3 (apparent stress at mid-gap due to the sheared fluid in the present apparatus) are roughly between 1·4 and 2 times higher than those of curve 4. The difference is probably due to two causes. First, there is the obvious

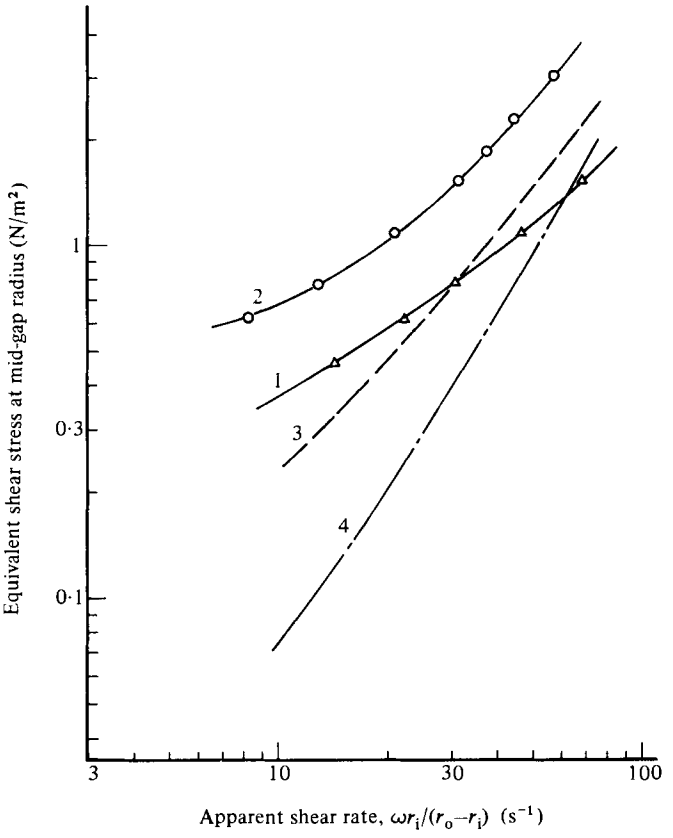

FIGURE 5. Typical calibration (plain fluid only) test results compared with empirical correlation of Bilgen & Boulos (1973). 1, no fluid in Couette device; 2, test with fluid; 3, test 2 minus test 1; 4, correlation of Bilgen & Boulos.

contribution from the sheared fluid in the bottom cavity underneath the inner cylinder. A second possible reason is that the inner cylinder becomes buoyant when the shear space is filled with water, decreasing the friction on the bottom conical bearing but more than making up for this loss by an increase in friction on the upper bearing.

For most of the data to be presented for the grain stresses, we have subtracted the total plain-fluid applied torque (corresponding to curve 2 of figure 5) from total torque applied to shear the suspension. This means that we have subtracted the full plain fluid shear stress τ_f from the total shear stress for the suspension to get the grain shear stress τ rather than subtracting only the fraction $\tau_f/(1+\lambda)$ as Bagnold did. This departure from Bagnold's approach was made largely for expediency. Because of the large values and fluctuations in machine friction, and the effects of the water in the lower cavity and buoyancy as described above, it was difficult to obtain reliable values for the plain-fluid shear stress τ_f. Since at moderate and higher concentrations τ_f is very small compared with the grain shear stress τ, it seemed pointless to bother with fractions of τ_f. Thus we merely subtracted the total plain-fluid calibration applied torque from the total suspension applied torque for the determination of the grain shear stress τ. In order to make direct comparisons of our measured stresses with Bagnold's data later, we utilize the empirical equations of Bilgen & Boulos (1973) for τ_f.

Calibration runs with plain fluid only were performed before almost every run with

Experiment		r_i (mm)	r_o (mm)	$\frac{r_o - r_i}{r_m}$	Shear-gap height (mm)	Wall material: inner	Wall material: outer	Rotation mode
Bagnold (1954)		46·2	57	0·209	50	flexible rubber	smooth Perspex	inner fixed outer rotating
Present tests	smooth walls	29·4	46·9	0·459	88·9	anodized aluminium	anodized aluminium	outer fixed inner rotating
	rough wall	31·9	44·4	0·328	88·9	rough rubber	rough rubber	

TABLE 1. Comparison of Couette-flow devices used in Bagnold's (1954) and present experiments

Experiment		Spherical particle material	ρ_s (g/c^3)	mean d (mm)	$\frac{r_i - r_o}{d}$	Interstitial fluid	Range of ν	Range of N
Bagnold (1954)		paraffin wax and lead stearate mixture	1·0	1·32	8·2	water and water–alcohol–glycerol mixture	0·135–0·623	600–700
Present tests	smooth walls	polystyrene	1·029	0·97, 1·24, 1·78	18, 14·1, 9·8	salt water	0·429–0·570	25–487
	rough walls				12·9, 10·1, 7·0		0·312–0·540	15–490

TABLE 2. Comparison of suspensions and test conditions used in Bagnold's (1954) and present experiments

the suspension to check whether large changes in machine friction had occurred. In some cases, variations between runs of as much as 20–30 % in calibration torque were observed. To load the suspension, the shear cell had to be dismantled and reassembled prior to each run; this evidently resulted in variations in machine friction between runs. At the low concentrations and high shear rates, the total applied torque for the plain-fluid case is a significant fraction of the total torque applied to shear the suspension. Thus at low concentrations the grain stresses to be shown are uncertain because of possible errors in the determination of the machine friction. However, at the high concentrations, because of the large values of the grain stresses, any error in machine friction is far less important.

3. Experimental results and discussion

For ready reference, the geometries of the Couette flow devices, the materials used in the suspensions and the ranges of the test conditions corresponding to Bagnold's (1954) and the present experiments, are summarized in tables 1 and 2.

3.1. *Smooth-wall experiments*

With the cylindrical walls of the Couette device in the smooth condition, experiments were performed on suspensions of three sizes of beads. Four values of concentration, $\nu = 0{\cdot}330$, $0{\cdot}429$, $0{\cdot}530$ and $0{\cdot}570$ for each bead size were tested. Figures 6(*a–c*) show the grain shear stress at mid-gap radius (total equivalent shear stress minus the plain fluid shear stress) plotted versus the apparent shear rate $\omega r_i/(r_o - r_i)$ for various concentrations and sphere sizes. For the lowest concentration of 0·330 the total torque was only slightly different from the plain fluid calibration torque. The variations in machine friction between runs made the determination of grain shear stress for this low concentration quite uncertain; for this reason no measurements for $\nu = 0{\cdot}330$ are shown on figure 6. All of the tests are affected by the endwalls of the annular shear space, but it is difficult to assess the endwall contribution to the overall stresses.

Although each set of tests for a *given loading* of the shear cell with a suspension of a particular grain size and concentration yielded quite consistent results with little scatter, there were differences between *different loadings* of suspensions of ostensibly the same grain size and concentration. The stresses are very sensitive to the value of concentration; for example, the differences between the two sets of runs at $\nu = 0{\cdot}570$ shown in figure 6(*c*) could be caused by an error in measured concentration of less than 0·5 %. The differences could also be due to different particle arrangements or packings set up during the initial loading of the shear cell. Cheng & Richmond (1978) have also reported that repeat tests on different samples of the same suspension often do not give the same results, and that adjustments in packing arrangements during repeated tests with the same sample give rise to variations in stresses. They felt that it is so difficult to discriminate the very small changes in density which have such pronounced effects that these changes may never be directly measured but only inferred from the change in stresses.

The slopes of the curves of shear stress versus apparent shear rate plotted on log–log paper are between 1 (corresponding to Bagnold's (1954) macro-viscous regime) and 2 (corresponding to the grain-inertia regime). Bagnold defined a dimensionless shear rate group that was proportional to the ratio of inertia stress to viscous stress:

$$N = \frac{\rho_s \lambda^{\frac{1}{2}} d^2 \, dU/dy}{\mu}, \tag{4}$$

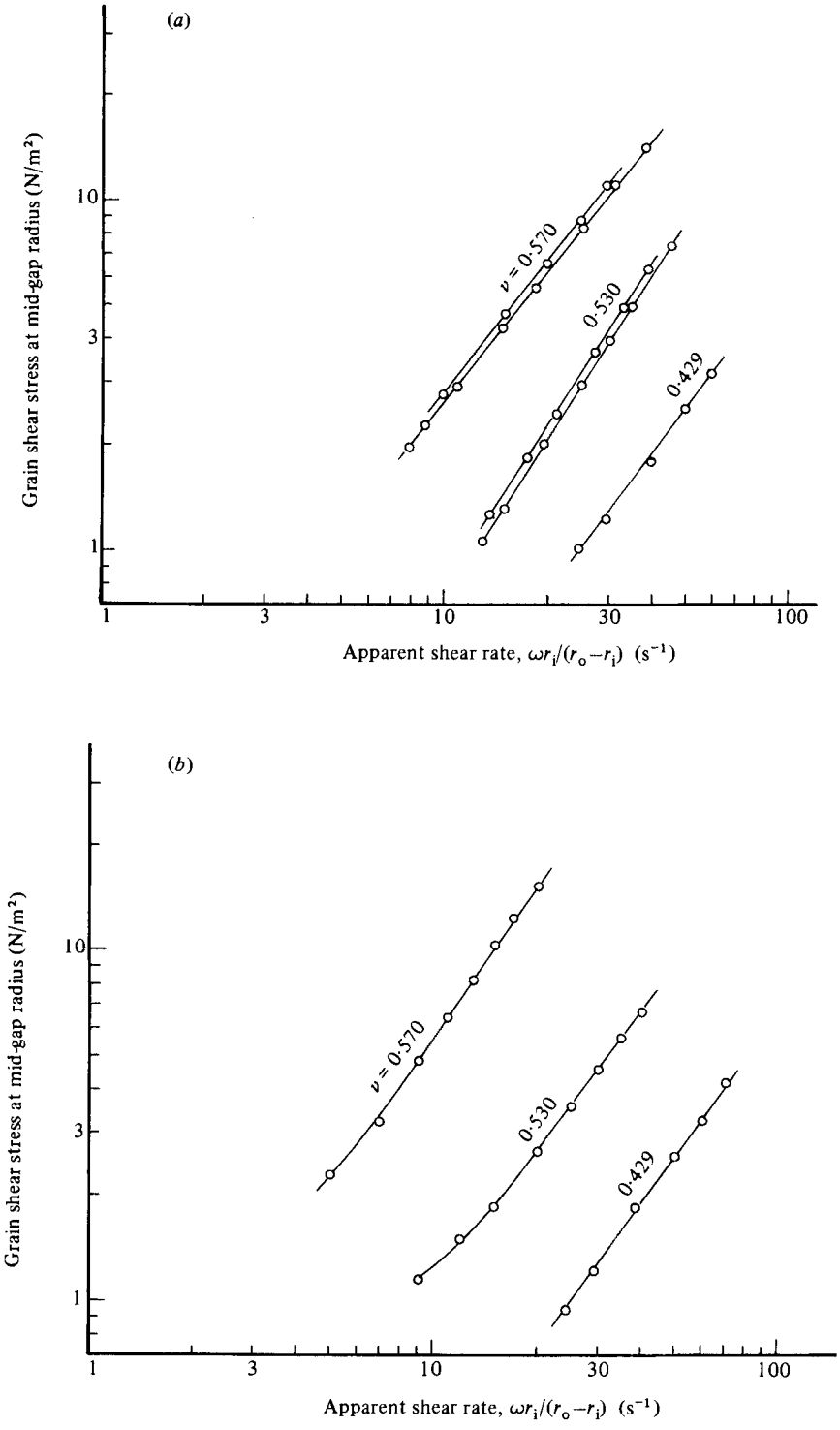

FIGURE 6(*a*, *b*). For caption see p. 464.

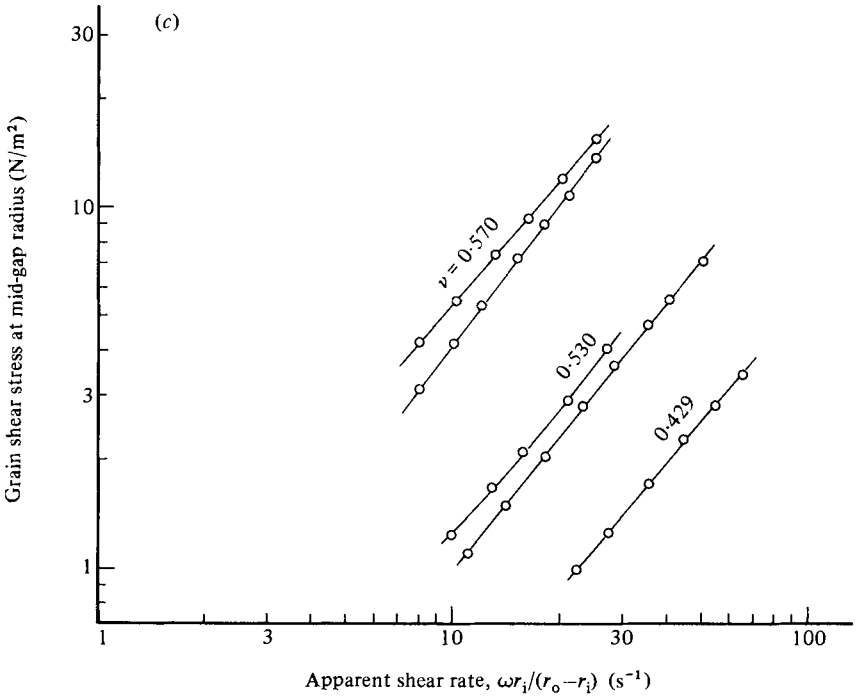

FIGURE 6. Smooth-wall test results for (*a*) 'small' ($d = 0{\cdot}97$ mm), (*b*) 'medium' (1·24 mm) and (*c*) 'large' (1·78 mm) beads. Full plain-fluid calibration stresses have been subtracted from total equivalent stresses to yield grain shear stresses shown.

where dU/dy is the apparent shear rate. In terms of N the transition between the viscous and inertia regions corresponded to values approximately between 40 and 450. The values of N for the present smooth-wall tests varied between 25 and 487. The slopes of the stress versus shear rate curves are thus consistent with the behaviour in Bagnold's transitional regime. It is also worth noting that, although Bagnold's experiments (with the outer cylinder rotating) showed that the plain-fluid ($\nu = 0$) shear stress varied as the square of the shear rate, in the present experiments (with the inner cylinder rotating) the plain-fluid shear stress varies as shear rate raised to a power somewhat less than 2 (see curves 3 and 4 of figure 5).

A comparison of the shear stresses measured in the present tests with those of Bagnold (1954) is shown in figure 7. Recall that the grain shear stresses shown on figures 6 were obtained by subtracting the full plain-fluid shear stress from the suspension shear stress. In order to make the present stress comparable to Bagnold's, we have added to the mean curves for each concentration shown on figure 6 a stress equal to $\tau_f/(1+\lambda)$, where τ_f is the plain-fluid shear stress calculated by the *empirical equations* given by Bilgen & Boulos (1973). Bagnold's stresses on the inner cylinder have been converted to values at the mid-gap radius by multiplying them by the ratio $(r_i/r_m)^2$. The densities of the suspensions used in the two different experiments were slightly different; 1·029 g/cm³ for the present tests and 1·0 for Bagnold's tests. Therefore, for the abscissa of figure 7, we have multiplied the apparent shear rate $\omega r_r/(r_o-r_i)$ by $S_g^{\frac{1}{2}}$, where r_r is the radius of the rotating cylinder and S_g is the specific gravity of the suspension. This is consistent with Bagnold's predicted behaviour in the grain-inertia regime; for the present comparison, using $S_g^{\frac{1}{2}}\omega r_r/(r_o-r_i)$ instead of simply $\omega r_r/(r_o-r_i)$ makes little difference because the fluid densities in the two experiments are nearly equal.

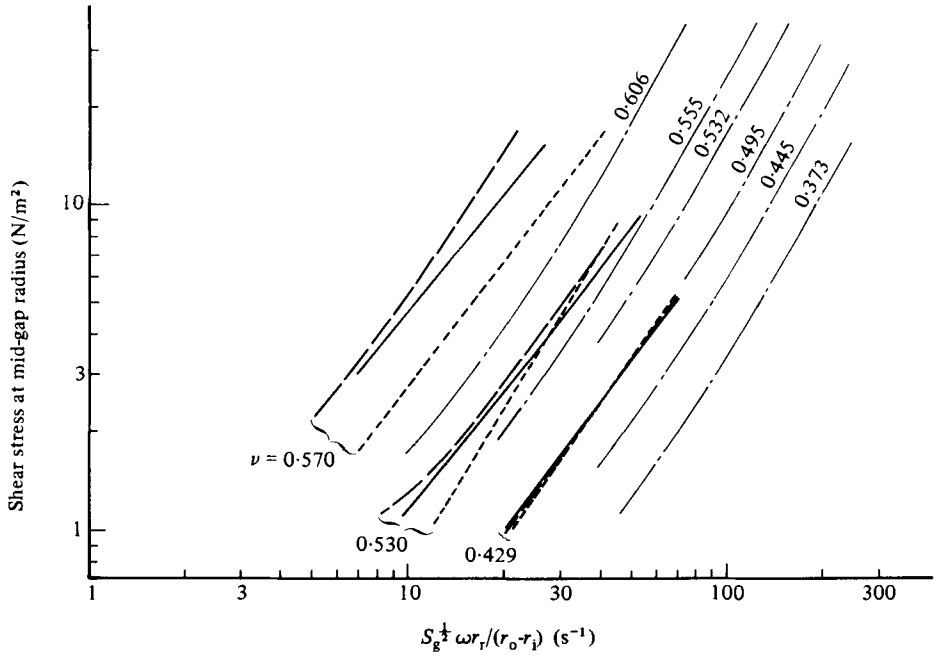

FIGURE 7. Comparison of present smooth wall results with Bagnold's (1954) data. To make the results comparable, $\tau_f\lambda/(1+\lambda)$ has been added to the mean test results of figure 6, and Bagnold's stresses have been converted to values at the mid-gap radius. ----, 0·97 mm beads; ---, 1·24 mm beads; ——, 1·78 mm beads; ———, Bagnold's data for 1·32 mm spheres.

The comparison in figure 7 shows the present stresses to be higher than those measured in Bagnold's apparatus. At least some of this difference can be attributed to the different roles with respect to rotation played by the inner and outer cylinders. In both sets of experiments the Taylor numbers were such that with plain fluid ($\nu = 0$) the flow was turbulent. For plain fluid, when the inner cylinder rotates, toroidal Taylor vortices form and the shear stresses can be considerably greater than those developed when the outer cylinder rotates (Taylor 1936; Bilgen & Boulos 1973; Fenstermacher, Swinney & Gollub 1979). One would expect the same general behaviour for non-zero concentrations.

The stresses in the present experiments also appear to increase more rapidly with concentration than do those in Bagnold's tests. This may be due to differences in cell-wall rigidities; the present Couette device had rigid aluminium cylinder walls, but Bagnold used a flexible rubber inner-cylinder wall. We attempted to perform tests at a concentration $\nu = 0{\cdot}602$ ($\lambda = 14$), but found that it was very difficult to load the shear cell with suspension at this high concentration. The annular gap is relatively narrow, and thus wall boundary effects reduce the possible packing concentration to something less than the maximum value of 0·637 for a dense random packing in an infinite container (Scott 1960). The maximum possible concentration in the finite gap may not have been much more than 0·602. After the cell was loaded it was found that the suspension could not be sheared. Although the inner cylinder could be rotated with some difficulty, the particles remained locked together and slip occurred right at the inner-cylinder wall. Evidently, in order to generate a shear within the suspension, dilation was necessary; but, because of the rigid wall, dilation was impossible. It may be that Bagnold was able to achieve shear at much higher concentrations ($\lambda = 14$–17) because he had a flexible inner-cylinder wall which could accommodate local dilation without a net overall expansion. It is quite possible that,

in the tests at higher concentrations in the present rigid-wall apparatus, intermittent locking or jamming of particles occurred giving rise to higher stresses than would be measured in Bagnold's apparatus where the wall could 'give' a little until the jam was overcome. In general, Bagnold's data also appear to be more consistent than the present tests as well as those of Cheng & Richmond (1978) and some unpublished tests in a different shear cell performed by one of the authors (S.B.S.) and coworkers; all of the latter tests were carried out in devices having rigid walls. The flexible wall may tend to eliminate finite particle diameter to shear gap ratio effects. There is also the possibility that, at higher concentrations, groups of particles locked together in rigid bands such that the actual shear took place over a gap *narrower* than the annular gap between the cylindrical walls of the apparatus. The actual shear rate would then be greater than the apparent shear rate one measures. The effects of such locking which *may* have occurred in both Bagnold's and the present experiments is discussed in Savage & Jeffrey (1981)†.

A further cause for the differences between the present measurements of stress and Bagnold's data may be the different elastic and frictional properties of the particles used in the two sets of experiments. Shen & Ackermann (1982) have developed an analysis for the stresses in a sheared 'granular fluid' which is similar in some ways to that of Savage & Jeffrey (1981) but treats the particle kinematics in a simpler way and includes the effects of the interstitial fluid and the material properties of the interstitial fluid. Their analysis shows that the stresses are sensitive to the coefficient of restitution and the Coulomb friction coefficient of the particles. It is likely that the paraffin-wax and lead-stearate beads used by Bagnold had a considerably lower coefficient of restitution e than the polystyrene beads used in the present experiments. The analysis of Shen & Ackermann (1982) predicts that such a difference in the es could cause a good part of the difference in the measured stresses.

At the lowest concentration shown in figure 7 the present tests show no apparent dependence of stress upon the particle diameter. Recall that a square-law dependence was predicted in the grain-inertia region. Note that the $\nu = 0{\cdot}429$ tests have the largest values of Bagnold's parameter N, but they are still in this transitional region where we might still anticipate some diameter dependence. It may be that at lower concentration the flow is not grossly different from the turbulent plain-fluid case. The presence of large amounts of interstitial fluid may damp the neutrally buoyant particles' motion to an extent such that they are unable to approach the interparticle dynamics that Bagnold associated with the grain-inertia region.

With increasing concentration the dependence of shear stress upon particle diameter emerges. At the two higher concentrations ($\nu = 0{\cdot}530$ and $0{\cdot}570$) the 'large'-size beads generally give higher stresses than the 'small' beads, but curiously in both cases the 'medium'-size beads yield the highest stresses. This anomalous behaviour could be due to irregular changes in machine friction combined with errors in the determination of concentration, but this seems unlikely to account completely for the observed differences. From figure 4 it may be seen that the gradations of the three sizes of beads are different. The 'medium' sized particles have a broader size distribution than either the 'small' or 'large' particles, and this *may* have affected the magnitude of the shear stresses developed. However, from the tests (§2.2.2) dealing with the packing characteristics the effects of size distribution would not appear to be very significant. The ratio of shear-gap width to mean particle diameter is 18·0, 14·1 and 9·8 for the 'small', 'medium' and 'large' diameter beads. It is quite

† Note that this paper contains an error in the definition of the Maxwellian velocity distribution function. One should replace v^2 by $\frac{2}{3}v^2$ everywhere in the paper.

possible that the gap width is small enough that finite-particle-size effects are becoming evident. At high concentrations it would seem reasonable that the suspension could be more readily sheared (with lower stresses being generated) if the particles can arrange themselves into an integral number of layers. If the gap width is increased or decreased so as to still include an integral number of layers at the same concentration and shear rate, then no large changes in stresses are expected. However, if the gap is changed by a fraction of one of these layer thicknesses then it seems likely that particle jamming and increased stresses would result. This mechanism is suggested as an explanation of the anomalous diameter dependence.

3.2. *Rough-wall experiments*

Figures 8(*a–c*) show grain shear stress versus apparent shear rate obtained in the experiments with the rubber roughness glued on the cylinder walls of the Couette device. Results are presented for the three different bead sizes and for concentrations of 0·312, 0·406, 0·491 and 0·540. The grain shear stresses were obtained in the same way as in the smooth wall case; the plain-fluid equivalent (hydrodynamic plus machine friction) shear stress at mid-gap radius was subtracted from the total equivalent shear stress. Generally the plain-fluid stresses were greater for rough walls than those for smooth walls, but the differences were the same order as the differences between runs resulting from machine-friction variations. The inner and outer radii used for the determination of the apparent shear rate $\omega r_i/(r_o - r_i)$ corresponded to the tops of the roughness elements. The roughness elements are large, and this creates uncertainties both in the concentration and the shear rate. The spacing of the cylindrical roughness elements is such that the small beads could move in and out through the troughs between the protuberances. On the other hand, the large beads often became wedged between the rubber roughness elements; this could be observed at the end of an experiment when the suspension was removed. The ambiguity in the choice of the appropriate annular gap width leads to uncertainties about the apparent shear rate. For example, if we choose the annular gap to lie between radii corresponding to the mid-heights of the roughness elements, the apparent shear rates are decreased by about 7 %.

Suspensions of particular concentrations were prepared in volumes equal to the total volume of the annular shear cavity with the roughness in place; these were then poured into the shear cell. Because of the local disturbances caused by the individual roughness elements the concentration appropriate for the sheared region may have been different from the overall mean concentration.

To make the comparison with Bagnold's (1954) data we have treated the data in the same way as in the smooth-wall tests. A fraction of the plain-fluid stress $\tau_f \lambda/(1+\lambda)$ was added to each of the mean curves for a given concentration obtained from figure 8; and Bagnold's stress at the inner cylinder was converted to stress at mid-gap radius.

In the rough-wall experiments (figure 8) the differences between individual runs at ostensibly the same test conditions were generally greater than those observed for smooth walls, and for the most part they increased with concentration and bead diameter. The variations in actual shear rate and concentration, which can be caused by the roughness elements as described above, no doubt contribute to these differences between tests.

The slopes of the stress–shear-rate curves in figure 8 are between 1 and 2; the data for the most part fall into Bagnold's transitional regime with the values of N ranging from 15 to 490.

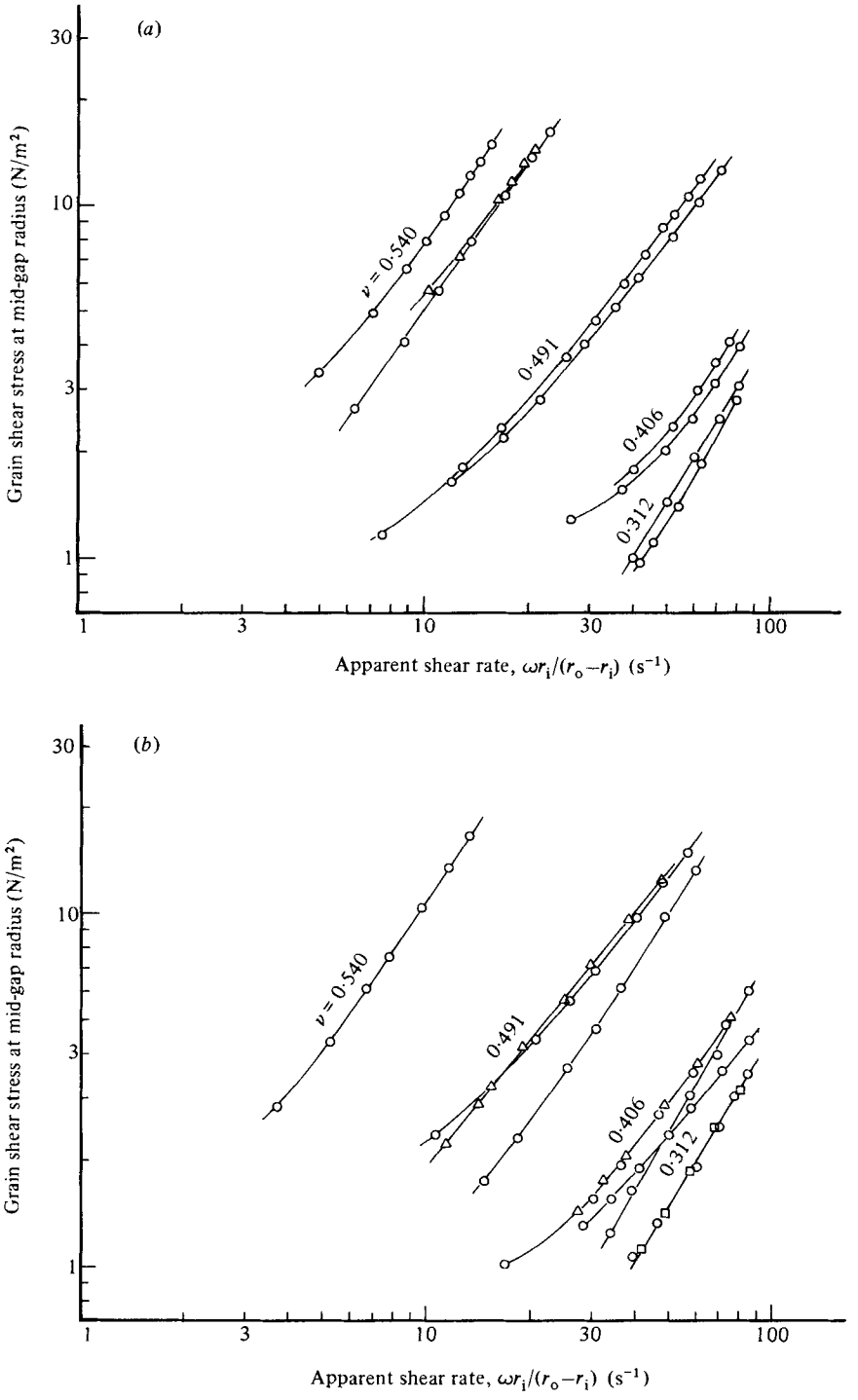

FIGURE 8(*a*, *b*). For caption see facing page.

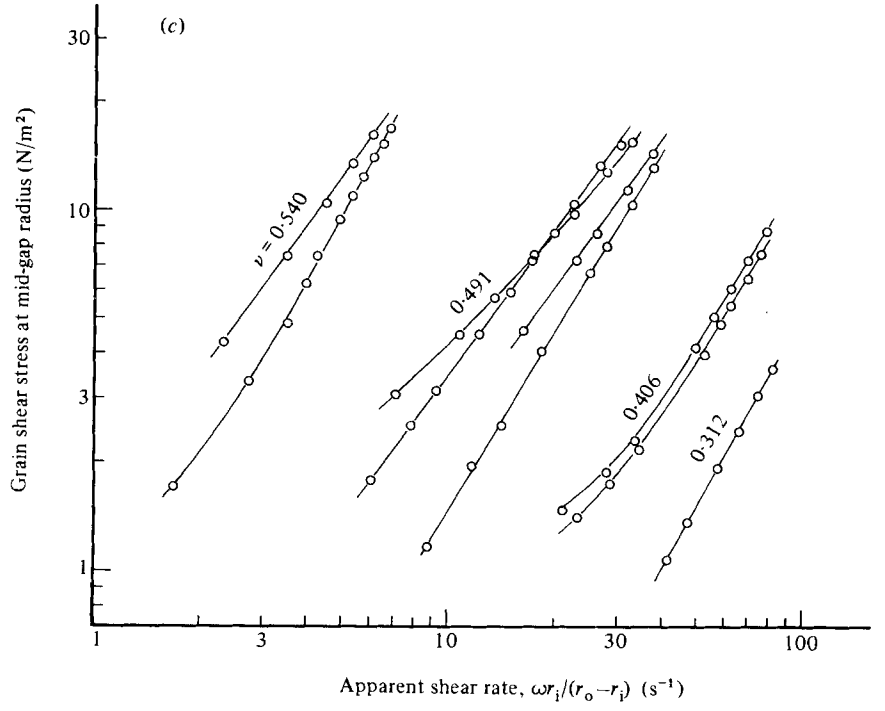

FIGURE 8. Rough-wall test results for (*a*) 'small' ($d = 0{\cdot}97$ mm), (*b*) 'medium' (1·24 mm) and (*c*) 'large' (1·78 mm) beads. Full plain-fluid calibration stresses have been subtracted from total equivalent stresses to yield grain shear stresses shown.

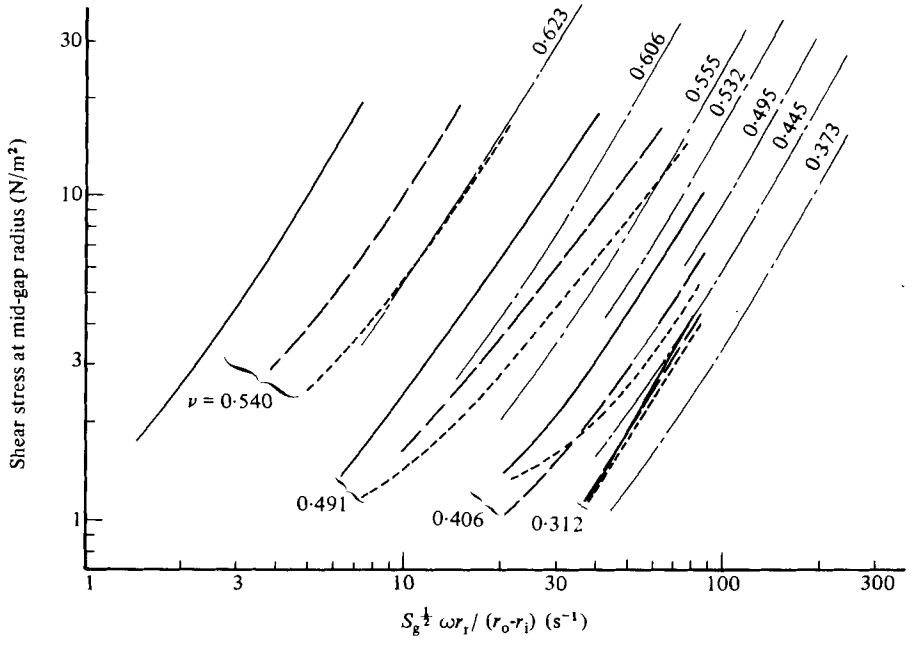

FIGURE 9. Comparison of present rough-wall results with Bagnold's (1954) data. To make the results comparable, $\tau_f \lambda/(1+\lambda)$ has been added to the mean test results of figure 10, and Bagnold's stresses have been converted to values at the mid-gap radius. -----, 0·97 mm beads; – – –, 1·24 mm beads; ——, 1·78 mm beads; ———, Bagnold's data for 1·32 mm spheres.

The rough-wall shear stresses were found to be higher than both the smooth-wall data and Bagnold's data (figure 9); the differences increased with increasing concentrations. The differences here suggest that, in the smooth-wall tests and Bagnold's experiments, 'slip' of the granules may have occurred. The solid particles next to the shear cell wall may have moved with a velocity different from that of the wall even though the no-slip condition was realized in the thin layers of interstitial fluid adjacent to the walls. Another reason for the difference could be that the roughness elements increase the vigour of the particle collisions and interactions. A recent analysis by Savage & Jeffrey (1981) for the shearing of dry granular material showed that at a given shear rate the stresses would increase with an increase in the magnitude of the particle fluctuations. This is analogous to the case in the kinetic theory of gases where the viscosity increases with temperature. Also, the normal-stress difference effects present in granulo-viscous flows (Savage 1979; Savage & Jeffrey 1981) could enhance the strength of the secondary flows associated with the toroidal Taylor vortices leading to larger shear stresses being required to rotate the inner cylinder.

As with the smooth-wall tests there is relatively little dependence of shear stress upon particle diameter at the low concentrations (figure 9). With increasing concentration this dependence increases to an extent such that, at a concentration of 0·540, the stresses depend more strongly upon particle diameter than the square-law dependence predicted by Bagnold for the grain-inertia regime. Again this may be associated with increased strength of the Taylor vortices generated by the roughness. Another possible explanation may be connected with curvature of the shear surfaces. The non-dimensional curvature, the ratio d/r_m of particle diameter to mid-gap radius, is about the same in the present tests with the small beads as in Bagnold's tests but is significantly larger for the medium and large beads. As the non-dimensional curvature of the shear surfaces increases, it seems likely that it would become more and more difficult to accommodate a shearing motion; i.e. the shear stresses are likely to increase.

4. Conclusions

Although it was not apparent at the outset of this investigation, it now seems that shear cell as well as the solid particles used in the present tests are sufficiently different from those used by Bagnold (1954) to make direct comparisons of measured stresses difficult. These differences, in both apparatus and results, have forced us to consider more thoroughly the mechanisms in operation during the rapid shear of a dense suspension; they also suggest a number of areas for more detailed study. In light of work now under way with J. T. Jenkins, D. J. Jeffrey and C. Lun (Savage 1982*a*, *b*; Jenkins & Savage 1982; Lun, Savage & Jeffrey 1983) to extend and generalize the analysis of Savage & Jeffrey (1981), it now seems inappropriate to attempt to determine unique values for the viscosity coefficients for dense suspensions in the way that one might do for a laminar Newtonian or even non-Newtonian fluid. In these theoretical developments, which at present neglect the interstitial fluid, the stresses (and hence the viscosity coefficients) depend upon the magnitude of the particle translational and rotational velocity fluctuations. These velocity fluctuations depend upon particle material properties and are governed by evolution equations, involving the production, diffusion and dissipation of fluctuation energy, which must be solved for each particular flow situation. Thus, the problem is analogous to certain approaches used to model turbulent Newtonian flows (see e.g. Reynolds 1976).

Generally, similar behaviour is to be expected for rapidly sheared suspensions of neutrally buoyant particles. Thus one might anticipate significant differences between two flows at the same shear rate involving particles of the same diameter and concentration if the overall flow geometry, boundary conditions and particle material properties (coefficients of restitution and surface friction, etc.) are different.

The present results suggest that, in general, the flow behaviour is rather more complicated than that pictured by Bagnold where he classified the flow as being of the macro-viscous, transitional or grain-inertia type depending upon the value of the dimensionless shear-rate parameter N. While the limiting behaviour in the macro-viscous and grain-inertia regimes seems well-founded, the precise definition of the borders separating the three flow regimes may not be so well-defined. For example, the present tests at the lowest concentrations, which correspond to the highest value of N and border on Bagnold's definition of the grain-inertia regime, show little dependence of shear stress upon particle diameter. On the other hand, at the highest concentrations, corresponding to lower values of N, there was a clear dependence of stress upon particle diameter. Bagnold argues that the stresses should depend upon the square of the particle diameter in the grain-inertia region. When the density of the interstitial fluid is very small compared with the solid particle density, the ideas about the generation of stresses by interparticle collisions and the dependence of the stresses upon the square of both particle diameter and shear rate can be valid as is shown by Bagnold's (1954) and Savage & Jeffrey's (1981) analyses. When the interstitial fluid density is the same as that of the particles as in Bagnold's and the present tests, at the lower concentrations at least, the interstitial fluid is likely to play a more important role at high shear rates than Bagnold suggested. Here, the flow may not be too different in character from the plain-fluid turbulent-flow case. The fact that, with increasing shear rate, the stresses deviate from the linear dependence upon shear rate and tend to a square dependence *could* mean that the flow becomes more turbulent-like rather than that it strictly approaches the grain-inertia type of behaviour envisaged by Bagnold.

The present investigation points out the importance of the boundary conditions and the effects of finite ratio of particle diameter to gap width. With smooth walls, particle slip at the walls may have occurred, particularly at the higher concentrations. The rough walls probably increased the magnitude of the particle-velocity fluctuations and the strength of secondary flows and hence the measured shear stresses. At high concentrations, rigid zones of locked particles may have developed such that the actual shear took place in a layer thinner than the annular gap between the cylindrical walls, the actual shear rate then being greater than the apparent one. Also at high concentrations, intermittent locking or jamming of particles spanning the full width of the shear gap is likely to have occurred. Increases in measured stresses are more probable in a rigid-walled apparatus than in one with flexible walls where the wall can locally deform permitting the 'column' of jammed particles to 'pass through'.

Many questions remain unanswered and further tests in a larger apparatus capable of generating a wider range of shear rates are suggested. It would be useful to have the ability to rotate either the inner or outer cylinder in the same basic apparatus and to have some means to visualize the flow to investigate the development of Taylor vortices or other secondary flows and the possible formation of rigid zones.

Grateful acknowledgement is made to the Natural Sciences and Engineering Research Council of Canada for support of this work. We are indebted to Tony Sum for his careful construction of the Couette flow apparatus. S.B.S. thanks Professor

G. K. Batchelor for his kind hospitality at the Department of Applied Mathematics and Theoretical Physics, University of Cambridge, where an earlier version of this paper was completed. Some preliminary results of the work described in this paper were presented at the U.S.–Japan Seminar on Continuum-Mechanical and Statistical Approaches in the Mechanics of Granular Materials, Sendai, Japan, 5–9 June 1978 (Savage 1978).

REFERENCES

BAGNOLD, R. A. 1954 Experiments on a gravity-free dispersion of large solid spheres in a Newtonian fluid under shear. *Proc. R. Soc. Lond.* **A225**, 49–63.

BAGNOLD, R. A. 1966 The shearing and dilation of dry sand and the singing mechanism. *Proc. R. Soc. Lond.* **A295**, 219–232.

BILGEN, E. & BOULOS, R. 1973 Functional dependence of torque coefficients of coaxial cylinders on gap width and Reynolds number. *Trans. A.S.M.E.* I: *J. Fluids Engng* **95**, 122–126.

BROWN, R. L. & RICHARDS, J. C. 1970 *Principles of Powder Mechanics.* Pergamon.

CHENG, D. C.-H. & RICHMOND, R. A. 1978 Some observations on the rheological behaviour of dense suspensions. *Rheol. Acta* **17**, 446–453.

DEXTER, A. R. & TANNER, D. W. 1971 Packing density of ternary mixtures of spheres. *Nature, Phys. Sci.* **230**, 177–179.

FENSTERMACHER, P. R., SWINNEY, H. L. & GOLLUB, J. P. 1979 Dynamical instabilities and the transition to chaotic Taylor vortex flow. *J. Fluid Mech.* **94**, 103–128.

FINNEY, J. L. 1970 Random packings and the structure of simple liquids I. The geometry of random close packing. *Proc. R. Soc. Lond.* A **319**, 479–493.

GADALA-MARIA, F. 1979 The rheology of concentrated suspensions. Ph.D. dissertation, Stanford University.

JEFFREY, D. J. & ACRIVOS, A. 1976 The rheological properties of suspensions of rigid particles. *Am. Inst. Chem. Engng J.* **22**, 417–432.

JENKINS, J. T. & SAVAGE, S. B. 1982 A theory for the rapid flow of identical, smooth, nearly elastic spherical particles. Submitted to *J. Fluid Mech.*

LUN, C., SAVAGE, S. B. & JEFFREY, D. J. 1983 The stresses developed during the simple shear of a granular material comprised of smooth, uniform inelastic spherical particles. (In preparation.)

REYNOLDS, W. C. 1976 Computation of turbulent flows. *Ann. Rev. Fluid Mech.* **8**, 183–208.

SAVAGE, S. B. 1978 Experiments on shear flows of cohesionless granular materials. In *Proc. U.S.–Japan Seminar on Continuum-Mechanical and Statistical Approaches in the Mechanics of Granular Materials, Sendai, Japan, 5–9 June*, 1978 (ed. S. C. Cowin & M. Satake), pp. 241–254. Tokyo: Gakujutsu Bunken Fukyukai.

SAVAGE, S. B. 1979 Gravity flow of cohesionless granular materials in chutes and channels. *J. Fluid Mech.* **92**, 53–96.

SAVAGE, S. B. 1982*a* Granular flows at high shear rates. In *Theory of Dispersed Multiphase Flow* (ed. R. E. Meyer). Academic.

SAVAGE, S. B. 1982*b* Granular flows down rough inclines. In *Proc. U.S.–Japan Seminar on New Models and Constitutive Relations in the Mechanics of Granular Materials, Cornell Univ., Ithaca, N.Y.* (ed. J. T. Jenkins & M. Satake). Elsevier.

SAVAGE, S. B. & JEFFREY, D. J. 1981 The stress tensor in a granular flow at high shear rates. *J. Fluid Mech.* **110**, 255–272.

SHEN, H. & ACKERMANN, N. L. 1982 Constitutive relationships for fluid–solid mixtures. *J. Engng Mech. Div. A.S.C.E.* **108**, 748–763.

SCOTT, G. D. 1960 Packing of equal spheres. *Nature* **188**, 908–909.

TAYLOR, G. I. 1936 Fluid friction between rotating cylinders. Part I. Torque measurements. *Proc. R. Soc. Lond.* **A157**, 546–564.